THERMAL PROPERTIES OF SHAFT FURNACES FOR EXPERIMENTAL ARCHAEOMETALLURGY

[1]Jan RŮŽIČKA, [1]Marek VELIČKA, [1]Mario MACHŮ, [1]Jana RŮŽIČKA, [1]David RIGO

[1]VSB - Technical University of Ostrava, Ostrava, Czech Republic, EU, ruz0048@vsb.cz

https://doi.org/10.37904/metal.2024.4927

Abstract

This paper is focused on the thermal properties of historical La Tène furnaces for the processing of iron ore. The technology itself has been used since 450 BC. It is an examination of the early technologies of iron production. This technology was mainly used in Central Europe by the Celtic tribes. Celtic people were well-known for iron making and, if not for the Roman Empire, the Celtic nation could dominate all of Europe. Via research work high number of experiments was made. There were many experiments with different starting properties and different conditions. This paper is primarily oriented towards the thermal properties of a furnace replica. Heat properties were examined. The experimental furnace which was fitted with thermocouples was studied thoroughly. There were twenty thermocouples in total installed. These thermocouples were installed in two layers. Other thermocouples were installed at the top, bottom, and inner end of the tuyere. Subsequently, the chemical properties of the slag were investigated and compared with historical findings. In this case, a striking similarity with the preserved findings was confirmed. Diffraction and fluorescence methods of examination of the samples were used for the analysis. Finally, the iron bloom and its chemical composition were investigated via SEM technology.

Keywords: Archaeometallurgy, metallurgy, thermal properties, La Tène period, shaft furnace

1. INTRODUCTION

Archaeometallurgy is a field focused on the early and primary period of metal processing. In terms of the focus of this work, iron is the most interesting one. Since its discovery, iron has been the most important metal. And to this day still probably is the most important material known to mankind. Nowadays it is taken for granted. In addition, the discovery and use of iron led mankind to many important milestones that changed the course of history [1, 2].

An important aspect is the monitoring of the products of the melting itself. Our ancestors were able to estimate the quality of the iron and the success of the process itself by the behavior of the slag [3]. Metallurgical processes are similarly governed today. Specialized programs can store large amounts of process information in memory. From those then infer adjustments to the metallurgical process itself. It is important to trace the beginnings of iron processing. The knowledge that countless finds will provide us, and especially our personal experiences, are irreplaceable [4, 5].

The main difference of past and present in smelting technology is heat [6]. Overall, every thermal aspect of smelting process had to be perfected to establish technology that is known today. Focus of this paper is on these thermal aspects of smelting process. The furnace was fitted with thermocouples to better define inner conditions of historical iron reduction process [7]. After completing experiment iron bloom and slag was tested and compered to findings to establish similarities. Diffraction and fluorescence methods of examination of the samples were used for the analysis. Finally, the iron bloom and its chemical composition were investigated through SEM technology.

2. EXPERIMENT

To measure the heat transfer parameters through the wall, the furnace wall was fitted with thermocouples from the inside and outside. The width of the wall was carefully shaped according to the initial requirements. To graphically represent the temperature, drop in the flue gas stream towards the wall, the furnace was fitted with thermocouples. These were placed at the same height on the inner wall and in the axis of the furnace. Two planes were measured in this way. Next, the temperature was measured in the hearth, right below the mouth of the nozzle. In total, the furnace was equipped with 19 thermocouples. It was type K for measuring lower temperatures and type R for higher temperatures. **Figure 1** shows the whole assembly of the experiment. Dots represent thermocouples locations, red for type K and blue for type R [8].

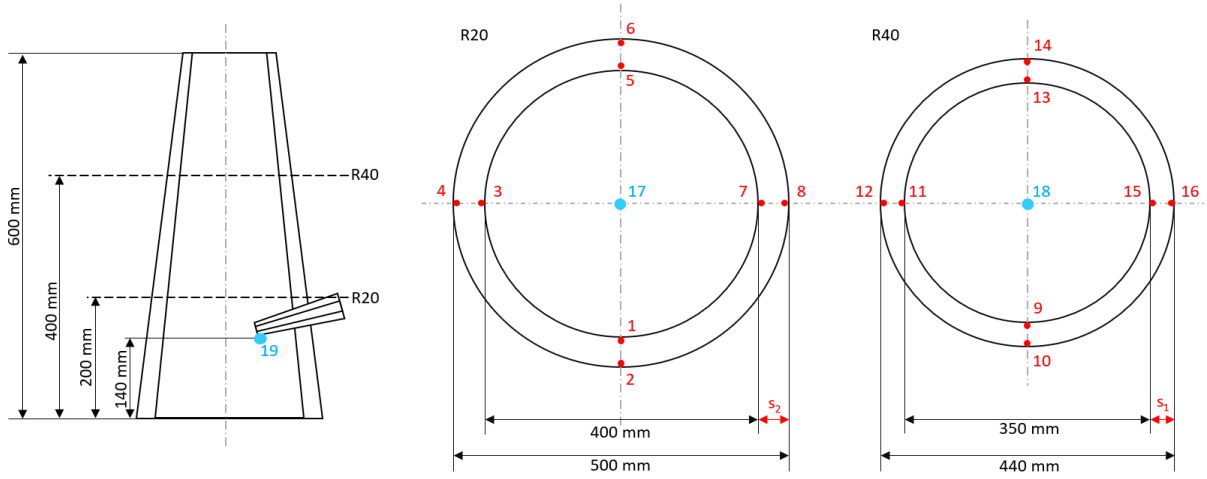

Figure 1 The furnace assembly with thermocouples and size parameters.

With the help of thermocouples, which were placed in the inner and outer sides of the furnace wall, it was possible to measure temperatures over time. These temperatures were used to calculate the heat flux q as in the next equation (1).

$$q = \lambda \frac{\Delta T}{s} \tag{1}$$

where:

q – heat flux (W·m^{-2})
λ – thermal conductivity (W·m^{-1}·K^{-1})
ΔT - temperature difference in K
s – wall thickness

Heat flux was measured in time of the whole process. The thickness of the wall was measured as: s_1 = 45 (mm); s_2 = 50 (mm). Average q was calculated for every two thermocouples in wall in both heights and are completed in the next **Table 1** for R20 and **Table 2** R40.

Table 1 Heat flux for thermocouples in 200 mm.

Δq	Δq_1	Δq_2	Δq_3	Δq_4
(W·m^{-2})	4381	4408	6180	4586

Table 2 Heat flux for thermocouples in 400 mm.

Δq	Δq_5	Δq_6	Δq_7	Δq_8
(W·m^{-2})	3357	4859	4775	4270

The heat flux progress for both measured planes R20 and R40 is recorded in **Figure 2** and **Figure 3.**

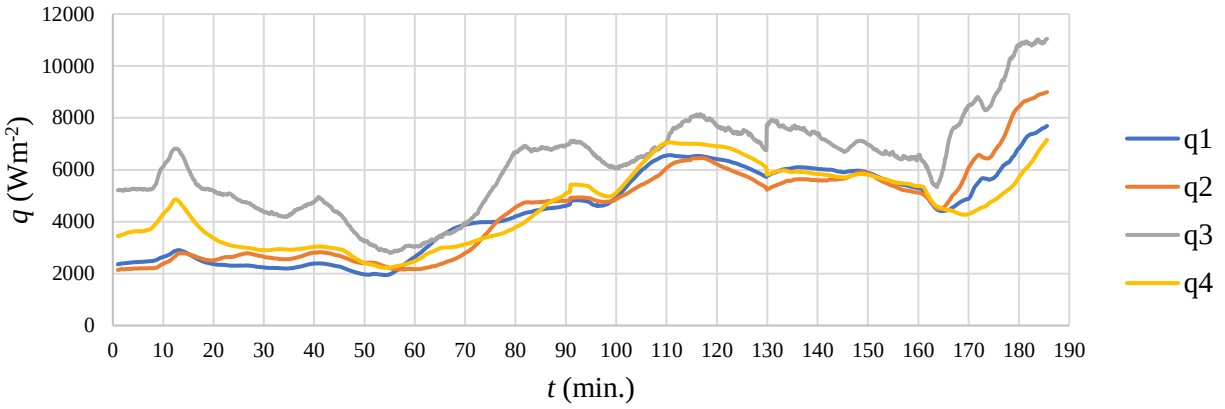

Figure 2 Heat flux progression in plane R20.

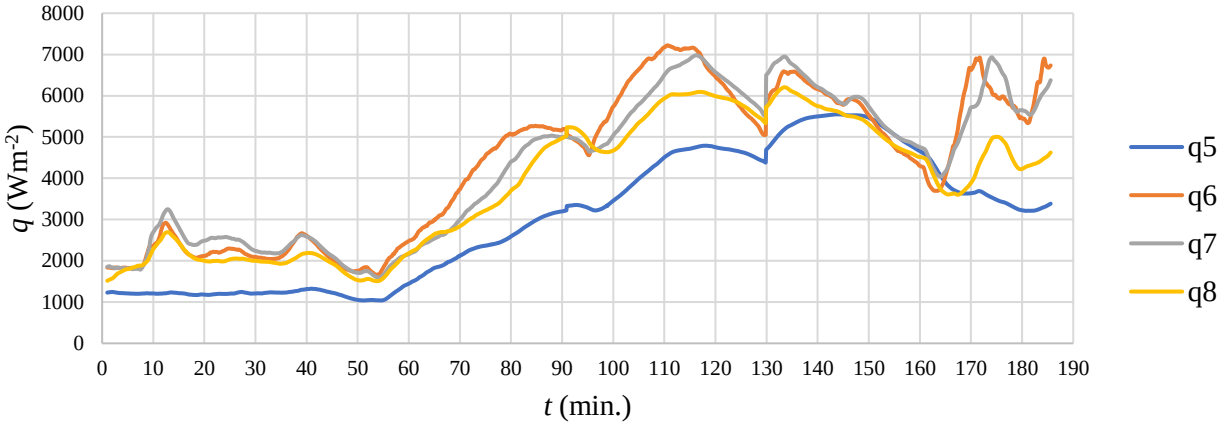

Figure 3 Heat flux progression in plane R40.

The development of heat flux is broadly similar. All curves show fluctuations in the same time windows. The mutual similarity of the curves q_1, q_2 and q_4 is clearly visible, they show broadly similar values. Heat flux of q_3 is shows the highest values. The temperature of the shaft gases and the heat contained in them is physically directed along the inside of the rear wall of the furnace. This effect is caused by the one-sided access of blown air into the furnace shaft. This is the opposite effect to the wall effect. The wall phenomenon occurs when the nozzle is too short and consequently the shaft gases flow along the inside of the front wall.

In R40 in general the heat flux of all sides of the furnace was about half lower than in the R20 plane. This is a completely logical matter since the shaft reducing gas has already cooled significantly during the previous passage through the furnace. An increase in values between 50 and 110 minutes can be spotted. Even though sudden drops occurred again afterwards, it is clear, that in this time the furnace reached a steady state in this plane.

The q_5 curve seems inappropriately monotonous. Undoubtedly, this is the result of greater thermal protection. So, either an element that increased the insulating properties stuck to this thermocouple, or the thermocouple was not properly shoved in the protective ceramic tube.

3. SLAG ANALYSIS

The chemical composition of the slag was measured using X-ray diffraction analysis. The selected 3 slag samples were photographed, ground and X-ray diffraction analysis was performed on a Rigaku MiniFlex instrument. X-ray diffraction determines the differences in individual samples. In this case, it would be possible to compare up to eight samples. In the case of Experiment 22, three samples were selected, and a comparison of their diffraction curves is shown in **Figure 4** below.

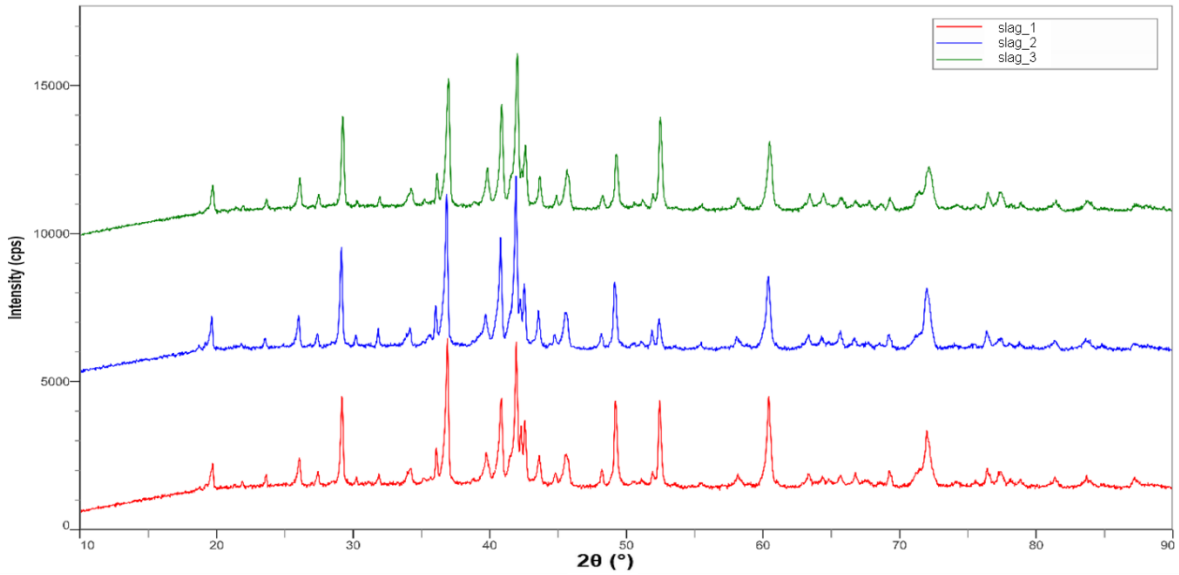

Figure 4 X-ray diffractogram of three slag samples.

Even after a quick evaluation, clearly all samples show a similar chemical spectrum. All the peaks are at the same angular values and their intensities differ only very slightly. From the same three slag samples, X-ray fluorescence analysis of the chemical composition was implemented. Instrument used was a compact Rigaku Supermini200. The mentioned device can perform complex analyses of matrix materials. The following **Table 3** shows the chemical composition of the slag from the experiment.

Table 3 Chemical composition of the slag samples from the experiment.

	MgO	Al_2O_3	SiO_2	P_2O_5	SO_3	Cl	K_2O	CaO
n	**wt%**	**wt%**	**wt%**	**wt%**	**wt%**	**wt%**	**wt%**	**wt%**
1	0.5915	4.8294	15.7513	0.2728	0.2119	0.0059	1.1971	3.8011
2	0.4511	4.9858	15.4416	0.281	0.0854	0.002	1.2224	4.1881
3	0.4129	3.8817	12.8078	0.2752	0.0791	0.0024	0.9313	3.5865
Average	**0.4852**	**4.5656**	**14.6669**	**0.2763**	**0.1255**	**0.0034**	**1.1169**	**3.8586**
	TiO_2	Cr_2O_3	MnO	Fe_2O_3	Co_2O_3	SrO	ZrO_2	LOI
n	**wt%**	**wt%**	**wt%**	**wt%**	**wt%**	**wt%**	**wt%**	**wt%**
1	0.2133	0.0355	0.1053	63.6825	<0.001	0.0143	0.0081	9.28
2	0.2525	0.0303	0.1253	65.072	<0.001	0.0217	0.0108	7.83
3	0.1733	0.0299	0.1045	67.1599	0.0605	0.0161	0.0088	10.47
Average	**0.2130**	**0.0319**	**0.1117**	**65.3048**	**0.0605**	**0.0174**	**0.0092**	**9.1933**

The second most dominant component is silicon dioxide. Silica sands are added to the loam clay mixture and are an integral part of the process. During reduction in the furnace, they also serve as additional slag-forming media that adjust the basicity of the slag. Furthermore, the content of aluminum oxide is visible, which was also introduced into the slag from the clay mass. Fluxes originating from charcoal are also present in the slag, which simplify the reduction process. Namely, it is potassium oxide and calcium oxide. The results were similar with findings presented in [3].

4. IRON BLOOM ANALYSIS

Reconstructive melts trying to mimic historic technologies are usually accompanied with material analysis [9] so altogether 5 measurements of one iron bloomer sample were made. SEM analysis from the surface of the sample in a limited area was concluded similarly to [10]. In one case, there was a point measurement, which was carried out for measurement number 3. In the next **Figure 5**, the sample for the second SEM analysis is visible, and the data collection points for the analysis are also shown here.

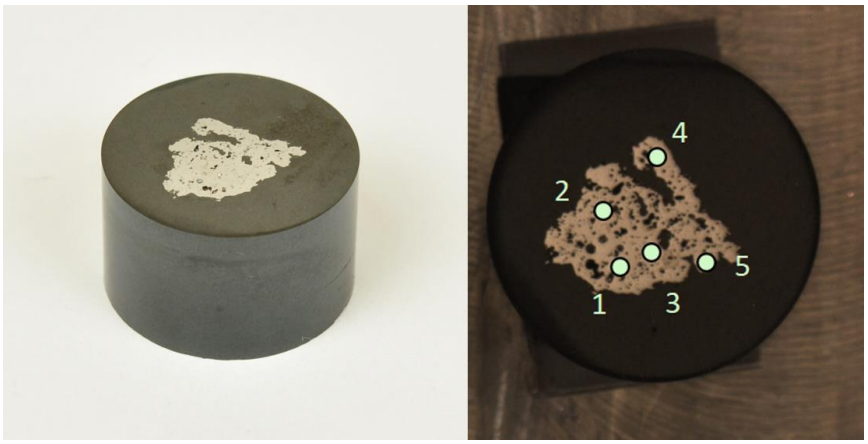

Figure 5 Prepared sample of iron bloomer with 5 measuring points.

The measured sample was very homogenic with high iron content. For measured points 1, 2, 4 and 5 was declared a **Table 4** lower. These values were stated separately because the whole measured area was without any dominant fluctuation. In measured point 3 was discovered an inclusion. This inclusion had proportionally different chemical composition. And in the table is marked as 3*.

Table 4 Chemical composition.

	wt%									
	Fe	C	Si	Ca	Mg	Al	K	Ti	Mn	O
1	98.9	0.9	0.2	-	-	-	-	-	-	-
2	99.1	0.8	0.1	-	-	-	-	-	-	-
3	99.0	0.8	0.2	-	-	-	-	-	-	-
3*	20.7	6.5	22.5	6.7	2.1	6.5	1.5	0.2	0.1	33.2
4	98.7	1.1	0.2	-	-	-	-	-	-	-
5	98.8	1.1	0.1	-	-	-	-	-	-	-

SEM analysis of this inclusion shows a high oxygen content that exceeds the amount of pure iron. Si. Ca. Al. C and Mg are also found here. The inclusion is most likely made of iron oxide, silica, and possibly iron carbide. Inclusion can be possibly a composition of more than one element stated above.

5. CONCLUSION

The experiments confirmed the uneven heating of the embedded material. Since the furnace is equipped with only one nozzle. there is one-sided air pressure and a forced flow of shaft gases through the charge. The stream of gases thus flows from the front wall towards the back wall. The rear wall thus heats up significantly more. The stream of shaft gases subsequently settles more towards the center when it travels a certain distance in the furnace. Stabilization occurs in 1/3 of the chimney, i.e. in the imaginary center of the furnace. This fact would be changed by means of a different shape of the nozzle. If the nozzle had a reduced outlet opening there would be an increase in pressure and consequently the air would be blown more towards the back wall of the furnace.

The chemical analysis of the slag first showed that the samples taken have practically the same chemical composition. even though they were taken from other parts of the furnace. The results of the chemical analysis itself showed a chemical composition that was very close to the chemical composition of similar slag findings. In addition. these slag finds appeared across historical periods.

Finally, the chemical composition of the iron bloomer was measured. After a very precise examination it turned out that the iron bloomer in question has a very homogeneous character. The measurement was carried out several times to confirm all the results that were obtained. The sample showed a high amount of iron. The Fe content ranged from 90 to 99%. Which is very remarkable for the historical production methodology that is almost 3000 years old. The main minor chemical components included carbon with contents from 0.6 to 2%. The occurrence of the chemical elements Si, Al, O, K and Ca was recorded both in significant and trace amounts.

ACKNOWLEDGEMENTS

This paper was created as part of the project No. CZ.02.01.01/00/22_008/0004631 Materials and technologies for sustainable development within the Jan Amos Komensky Operational Program financed by the European Union and from the state budget of the Czech Republic and was supported under Project No. SP2024/025 - Advanced materials and technologies for decarbonization.

REFERENCES

[1] HLAVA. M., VÍCH. D. Laténské osídlení Boskovická. Pravěk. Supplementum 17. 2007. 11-86. ISSN 8086399338.

[2] ORFANOU, V. Early iron age greece: Ancient pherae and the archaeometallurgy of copper. *Aegis: Essays In Mediterranean Archaeology*. 2015. 107-116. ISSN 9781748912017.

[3] HEEB. J., OTTAWAY. B. Experimental Archaeometallurgy. In: *Archaeometallurgy in Global Perspective*. New York: Springer. 2014. 161-192. ISBN 978-1-4939-3357-0.

[4] PLEINER, R. Iron in archaeology: the Early iron age european bloomery smelters. *Praha: Archeologický ústav AV ČR*. 2000. ISBN 80-86124-26-6.

[5] RŮŽIČKA. J., MACHŮ. M., HAŠČIN, J. Archaeometallurgy – experimental ferrous metalurgy. *In: Proceedings 29th International Conference on Metallurgy and Materials*. Brno: 2020. 144-149. ISBN: 978-80-87294-97-0.

[6] LARREINA-GARCÍA, D., YANXIANG, L., LIU, Y., MARTINÓN-TORRESET, M. Bloomery iron smelting in the Daye County (Hubei): Technological traditions in Qing China. *Archaeological Research in Asia*. 2018. **16**. 148-165. ISSN 2352-2267.

[7] ERB-SATULLO, N., and WALTON. J. Iron and copper production at Iron Age Ashkelon: Implications for the organization of Levantine metal production. *Journal of Archaeological Science: Reports*. 2017. **15**. 8-19. ISSN 2352-409X.

[8] MAIA, R. R., DIAS, M. S., de FARIAS AZEVEDO, C., R. Archaeometry of ferrous artefacts from Luso-Brazilian archaeological sites near Ipanema River. Brazil. In: *Revista Escola de Minas*. Ouro Preto: 2015 187–193.

[9] ALIPOUR R., REHREN T. Archaeology and alchemy applied: Experimental reproduction of Persian chromium crucible steel making. *Journal of Archaeological Science: Reports*. 2023. **47**.

[10] SERRANO S., RODRIGUES A., SILVA R.J.C., FIGUEIREDO E. Study of an Iron Age Gilded Silver Earring by XRF, SEM-EDS and Multifocus OM. *Heritage*. 2023. **6**(5). 4187 – 4201.